Polypropylene Surface Modification with Stearyl Alcohol Ethoxylates to Enhance Wettability

Vasantha M. Datla, Eunkyoung Shim, Behnam Pourdeyhimi

College of Textiles, North Carolina State University, Raleigh, North Carolina 27695-8301

Received 16 February 2008; accepted 30 June 2009
DOI 10.1002/app.31051
Published online 3 March 2011 in Wiley Online Library (wileyonlinelibrary.com).

ABSTRACT: Stearyl alcohol ethoxylated additives were melt-blended in polypropylene (PP) films, and the characteristics of the modified films were investigated. The melt blending of stearyl alcohol ethoxylates improved the hydrophilicity of the PP films through additive surface segregation. Surface specific techniques, such as X-ray photoelectron spectroscopy and time-of-flight secondary-ion mass spectrometry, were used to study the surface compositions of the samples modified with ethoxylated additives. This revealed that the surface concentrations of the additives were significantly higher than the bulk concentrations in all samples. In addition, the surface compositions of the additive-modified samples continuously changed, even after the films were fully solidified. We also found that the resulting surface characteristics were very dynamic, so the melt-additive-containing polymer surfaces responded to water exposure, and their surface properties and morphologies were altered as a result. © 2011 Wiley Periodicals, Inc. J Appl Polym Sci 121: 1335–1347, 2011

Key words: additives; blends; poly(propylene) (PP); surfaces

INTRODUCTION

One of the most important surface characteristics of a fiber is its wettability or the hydrophilicity of its surface, which affects the liquid transport properties, absorbency, hand, and comfort of the product.[1] Polypropylene (PP) fibers, with their low cost; desirable mechanical, physical, and thermal properties; and growing commercial applications, are widely used to make both woven and nonwoven fabrics, such as carded web, spun-bond, melt-blown, or composite fabrics.[2] However, the highly hydrophobic nature of the PP surface is its major drawback for many applications, including hygiene, medical, and filtration applications. A few examples where the use of PP with an improved hydrophilicity can add more value are diaper coverstocks, industrial sorbents and wipes, battery separators, carpet backings, and components of breathable composites.[3,4]

Frequently used hydrophilic surface modification methods for PP include topical finishing[5] and plasma, corona, and flame treatments. All of these methods lead to an immediate hydrophilicity that deteriorates over time.[6,7] Also, each of these methods has several disadvantages concerned with the processing and durability. It has also been reported that a hydrophilic surface can be obtained by chemical surface derivatization, such as by graft polymerization, but PP is one of the polymers most resistant to chemical modification.[8–10] Therefore, normally necessary treatment conditions can lead to the degradation of the polymer.[5]

The process of the melt blending of surface-segregating additives in the host polymer is a promising method for improving the surface properties of fibers in many applications. The process consists of melt-blending the additive with the host polymer, extruding a fiber or a film, and allowing the additive to bloom to the surface of the product. The transfer of additives from the bulk to the surface, sometimes called *blooming* or *surface migration,* is crucial in this process because it enables the polymer to achieve desirable surface properties with a low concentration of additives and without alteration of the bulk properties. It has been reported that PP nonwoven fabrics produced with an ethoxylated melt additive did not adversely affect the tenacity of fabrics.[11] To perform as a melt additive that is able to modify surface properties, physical processes, such as surface segregation, shear, and diffusion, can be used to transport the additive to the polymer surface.[12] It has been suggested that the migration mechanism is based on the surface tension gradient, molecular weight differences, and other polymer–additive interactions.[13,14] Despite the method's appeal, there has been surprisingly little fundamental research conducted to establish principles for additive selection and for optimizing the processing conditions to enhance the transport of surface-functionalizing additives in polymeric hosts.[16]

Correspondence to: E. Shim (eshim@ncus.edu).
Contract grant sponsor: Nonwovens Cooperative Research Center (North Carolina State University, Raleigh, North Carolina).

TABLE I
Melt Additives with Their Chemical Structures, HLBs, and O/C Ratios

Name	Melt additive	Chemical structure	HLB[a]	O/C (mol %)
POE2C18	POE 2 stearyl alcohol (Ethal SA-2)	$CH_3(CH_2)_{16}CH_2(OCH_2CH_2)_2OH$	5.9	14
POE4C18	POE 4 stearyl alcohol (Ethal CSA-4)	$CH_3(CH_2)_{16}CH_2(OCH_2CH_2)_4OH$	8.7	19
POE6C18	POE 6 stearyl alcohol (Ethal SA-6)	$CH_3(CH_2)_{16}CH_2(OCH_2CH_2)_6OH$	10.5	23

[a] The data were calculated using Griffin method.[15]
[b] POE, polyoxyethlyene.

In this article, we report the effect of melt-additive composition and characteristics on the hydrophilic surface modification of PP. The migration behavior and surface hydrophilicity at the initial stage and after aging, the relation between the migration rate and the chemical structure, and the durability against water contact were studied and analyzed for PP with stearyl alcohol ethoxylated additives.

EXPERIMENTAL

Materials and sample preparation

Film-grade PP resin with a melt flow index of 18 (supplied by Goulston Technologies, Monroe, NC) and stearyl alcohol ethoxylate additives, listed in Table I, were melt-blended and extruded into films with a twin-screw extruder in Polymers Center of Excellence (Charlotte, NC). Films produced by this procedure were referred to as POE2C18/PP, POE4C18/PP, and POE6C18/PP films in this study, and the additive concentration blended in samples was 2% (w/w) by the weight of the film. PP film with no melt additives was extruded under the same conditions to produce the control sample.

High-performance liquid chromatography (HPLC)

Reverse-phase HPLC was used for the separation of the ethoxylated additives to examine the distribution of the ethylene oxide chains length in the additives. The stationary phase used was a C-18 surfactant column (Acclaim surfactant column, Dionex, Sunnyvale, CA); this consisted of polar silica gel particles coated with nonpolar C-18 hydrocarbon. Water, acetonitrile, and methanol were used as the mobile phase, and a linear gradient was developed for the separation, as shown in Table II. The chromatographic separation was performed on a Waters 2695 instrument, and detection was done by evaporative light scattering (ELS 2420) (Waters, Milford, MA).

Differential scanning calorimetry (DSC) analysis and crystallinity measurement

Thermal analysis of the modified PP films was carried out on 3–5-mg samples in a power-compensated PerkinElmer Diamond DSC thermal analyzer (Waltham, MA). An indium standard was used for calibration, and nitrogen was used as the purge gas. The samples were heated at an underlying heating rate of 20°C/min from −50 to 200°C, and the thermal transitions in the samples are reported. The degree of crystallinity was evaluated by the ratio between the melting enthalpy of the film and the melting enthalpy of perfectly crystalline PP (50 cal/g).[17]

X-ray photoelectron spectroscopy (XPS)

XPS measurements were carried out in a RIBER LAS-3000 spectrometer (Bezons, France) with a monochromatic MgKα X-ray source (1254 eV), an electron multiplier as the detection system, and a hemispherical electron energy analyzer. The area analyzed on the sample surfaces was approximately 3 mm in diameter. A standard 75° takeoff angle (the angle between the surface normal and the axis of the analyzer lens) was used for the surface scans, which was believed to probe the outer 1–5 nm of the polymer surface. The surface oxygen content or O/C ratio (%) was calculated from the areas of the carbon 1s (C1s) and oxygen 1s (O1s) peaks in the survey spectra with CASA Software Ltd. (Teignmouth, UK). The relative sensitivity factors used were 2.85 and 1 for oxygen and carbon, respectively.[18,19]

Then, the surface oxygen content or O/C ratio (%) was further converted to molar melt additive surface concentration. According to the structure of the repeat units of PP and the molecular structure of the additives, the molar fraction of the melt additive surface concentration in the sample was calculated with the following equation:

$$\left(\%O/C_{\text{sample}} - \%O/C_{\text{PPControl}}\right) = \frac{X \cdot O_{\text{MeltAdditives}}}{X \cdot C_{\text{MeltAdditives}} + (1 - X)C_{\text{PP}}} \quad (1)$$

TABLE II
Mobile-Phase Gradient Program for the Separation of Stearyl Alcohol Ethoxylated Additives

Time (min)	Water (%)	Acetonitrile (%)	Methanol (%)
0	55	40	5
20	5	90	5
27	5	90	5
28	55	40	5
33	55	40	5

where X is the molar melt additive surface concentration in the blend film and $O_{MeltAdditives}$, $C_{MeltAdditives}$, and C_{PP} are the stoichiometric oxygen and carbon atomic concentrations in the pure melt additives and pure PP repeat unit, respectively. % O/C_{sample} and % $O/C_{PPControl}$ are the surface oxygen content of the sample and the PP control film, respectively, as measured with XPS. The O/C (%) contribution of the control PP film was subtracted from the surface O/C ratio (%) obtained in the melt-blended PP films to get a clear indication of the surface excess of the melt additive.

Time-of-flight secondary-ion mass spectrometry (TOF-SIMS)

The surface compositions of the melt-blended films were also analyzed with the TOF-SIMS method. All TOF-SIMS spectra were acquired with a PHI TRIFT I instrument (PHI, Chanhassen, MN) to raster a 100 × 100 μm^2 surface area with a 15-kV gallium (Ga^+) ion beam at a 600-pA current with an extraction voltage set at 7500 V. On the basis of the spectra results, the chemical mappings of the additive molecules on the sample surfaces were also carried out with high spatial resolution.

Water contact angle measurements

The water contact angles were measured with a zoom lens and a charged coupling device camera. Images of the deionized water droplets on the sample films were captured every 1/20 s to investigate the dynamic interactions between the water and the sample surface. The water contact angle was measured at different times up to 4 months after extrusion.

Atomic force microscopy (AFM)

AFM was used to explore the heterogeneity and morphology of the surface of additive-containing films and their impact on additive performance. Height images of the film surfaces were obtained and analyzed with a Nanoscope III Multimode AFM (Digital Instruments, Plainview, NY) in tapping mode.

Water immersion durability

Exposure of films to water may cause realignment and a loss of the additive molecules. Hence, the durability of the surface-modified PP film was evaluated by the immersion of a series of samples (1 g) in 200 mL of deionized water for 6, 12, and 24 h independently at room temperature in an incubator subjected to agitation (at 100 rpm). All of the samples were later air-dried and examined with XPS and water contact angle data.

After the samples were removed, the water solutions were analyzed for changes in the water surface tension for possible additive loss with the help of a Fisher Scientific (Suwanee, GA) surface tensiometer working on the DuNouy ring principle at room temperature.

RESULTS AND DISCUSSION

Additive characterization with reverse-phase HPLC

It is well known that most commercial alcohol ethoxylate additives are not pure components but contain molecules having different numbers of ethoxylate groups. This is because alcohol ethoxylates are prepared by the addition of ethylene oxide to aliphatic alcohols under base-catalyzed conditions, and the reactions result in polydisperse products having a distribution of the length of the ethoxylate groups. Because the length of the ethoxylate group affects key properties of the additive molecular characteristics, including the molecular size, hydrophilic/hydrophobicity of additives, water solubility, and surface adsorption properties, the determination of ethoxylate group length and ethoxylate group distribution is an important step in understanding the behaviors of the additives in surface modifications.[20,21]

Reverse-phase HPLC was used to examine the distribution of ethoxylate chain length in the additives used, and the analysis results are shown in Figure 1. The stearyl alcohol ethoxylate oligomers eluted according to the ethoxylate number. As the ethoxylate number increased, interactions of the additives with the nonpolar stationary phase became weaker, and the retention time decreased. Individual components with different ethylene oxide lengths in all three additives were well separated with the HPLC procedure used and provided a better understanding of the composition and hydrophilicity of the additives.

It revealed all three additives exhibited polydispersity with a distinct ethoxylate chain length distribution. The POE2C18 additive had a relatively large portion of compounds with a low degree of ethoxylation. It mostly comprised compounds with an ethoxylate number of 1–6, with a trace of other compounds, including nonreacted stearyl alcohol, with peaks around 21.5 min. This suggests that the POE2C18 additive was less hydrophilic compared to POE4C18 and POE6C18, which is an important factor in surface modification. The POE4C18 and POE6C18 additives had broad distributions, with ethoxylate numbers ranging from 1 to 9, and 2 to 13, respectively. POE6C18 contained a large portion of long ethylene oxide chains compared to POE4C18. Long ethylene oxide chains in the POE6C18 additive

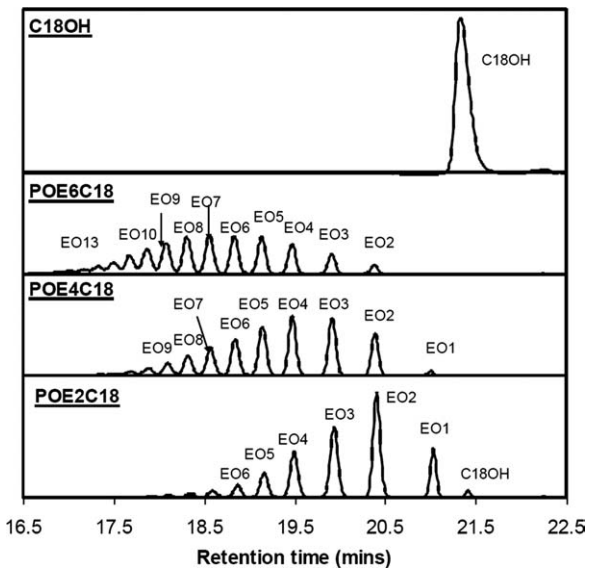

Figure 1 Reverse-phase HPLC chromatograms of stearyl alcohol ethoxylated additives used in the surface modification of PP. The chromatogram of Stearly alcohol standard (1-octadecanol, C18OH) is also shown.

made it comparatively more hydrophilic with a higher hydrophilic–lipophilic balance (HLB) value.

Additive surface segregation and migration behavior

The additive surface compositions were investigated with XPS, which provided quantitative analysis of the atomic composition of the surface by detection of the characteristic binding energies associated with each element with an analytical depth of approximately 1–5 nm.[1,20] In all melt-additive-containing films, peaks at about 530 and 285 eV were detected; these peaks corresponded to the characteristic binding energies of O1s and C1s, respectively (sample spectra shown in Fig. 2). The presence of peaks in these binding energy levels and their relative intensities indicated the addition of the additives in PP induced the remarkable increases in the surface oxygen content.

The surface oxygen content calculated from the XPS spectra are given in Figure 3. Although some surface oxygen was detected in the PP control film, as a result of oxidation and surface impurity, most of the oxygen detected could be attributed to the ethoxylated groups in the additives. Then, the melt-blending of ethoxylate additives created highly polar, oxygen-enriched surfaces. More interestingly, the surface oxygen contents detected were significantly larger than the values expected if the additives were uniformly distributed. Therefore, we concluded that the surface concentration of the additives was higher than that of the bulk and this was the result of additive surface segregation.

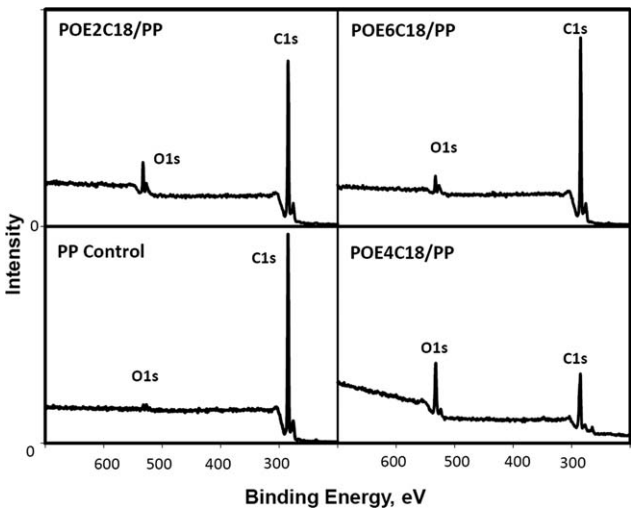

Figure 2 XPS spectra of the additive-modified films taken 3 weeks after extrusion.

The surface enrichments of stearyl alcohol ethoxylate melt additives could be more clearly understood when the O/C ratios (%) were converted to molar melt additive surface concentrations with eq. (1). The surface molar concentrations of the ethoxylated additives in the modified films ranged from 0.9 to 36%; these values were significantly higher than the bulk molar concentrations, which ranged from 0.37 to 0.56%, and corresponded to a 2% (w/w) concentration in all of the produced samples (Table III). Again, this demonstrated that the additives in the PP films were not uniformly distributed but highly concentrated on the surface and that additive-enriched polar surfaces were generated.

The causes of the surface enrichment of the ethoxylate additives could be complex. They could include polymer-additive phase separation caused

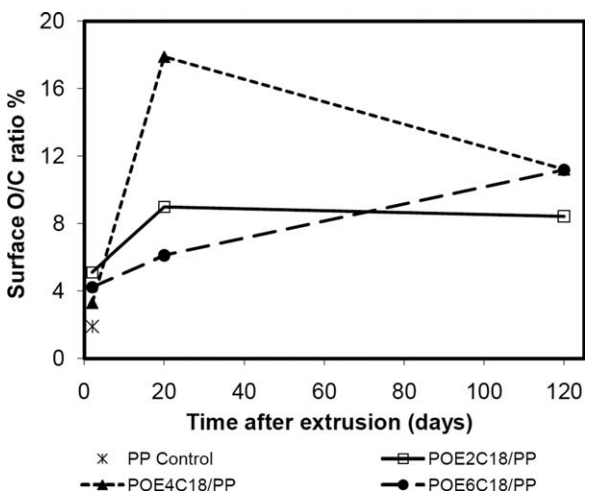

Figure 3 Surface O/C ratio (%) for the surface-modified films with ethoxylated stearyl alcohol melt additives measured 2 days, 3 weeks, and 4 months after the extrusion date.

TABLE III
Molar Surface Concentrations of the Ethoxylated Alcohol Melt Additives in the Modified PP Films Calculated by Means of Elemental O/C Ratios Derived from XPS Analysis

Film sample	Bulk molar concentration of the melt additive (%)	Molar melt additive surface concentration in the blend (%)		
		Day 2	Week 3	Month 4
POE2C18/PP	0.56	4.04	12.81	11.07
POE4C18/PP	0.45	0.90	36.33	9.75
POE6C18/PP	0.37	1.09	2.15	6.18

by immiscibility of the ethoxylate chain and PP molecules[21] and entropic preference of small molecules on the surface.[13,22] Hydrophilic ethoxylate groups in the additives had little affinity to the PP host polymers, which could drive additive molecules away from the PP host through migration to the surface or micelle formation. In contrast, hydrophobic C18 chains in the additives still provided affinity to the host PP polymers. The small molecular sizes of the additives further promoted surface segregation of the additives by entropic preference. It is well known that the configurational entropy per segment of polymer chains near rigid surfaces is believed to be substantially lower than that in bulk polymer systems.[13,22] Therefore, the polymer layer near the surface would be expected to be depleted with high-molecular-weight polymer components and enriched with lower molecular weight ones to reduce conformational entropic penalties at the blend surface.[13,14,22]

However, our observation showed that the equilibrium surface concentrations were not immediately achieved during the extrusion. Both Figure 3 and Table III illustrate that the additive surface concentrations continued to increase after extrusion and that the additives in the PP film had mobility even after the film was fully solidified. Then, the mobility of additives inside PP matrix could have been another important factor in the production of the polar surfaces.

Both the rate and the degree of additive surface segregation were affected by the distribution of ethoxylate group length in the additives because two main driving forces of the surface segregation, additive molecular weight and miscibility of the additives, were dependent on it. At day 2 after extrusion, the POE2C18/PP film showed significant higher level of surface segregation compared to the POE4C18/PP and POE6C18/PP films. The surface additive molar concentration of the POE2C18/PP film was more than seven times larger than that of the bulk concentration, whereas for the POE4C18/PP and POE6C18/PP films, the surface molar concentrations were only about two to three times the bulk concentration. This may have been the result of the faster migration of POE2C18 additive because of its high mobility in the PP matrix and because of the small molecular size and short ethoxylate chain length. Migration to the surface of other additives with long ethoxylate chain length may have been hindered by PP molecules and resulted in a delay in reaching equilibrium status. However, additives with long ethoxylated chains were eventually pushed out from the bulk of the PP polymer because of their more polar nature and poor compatibility with the PP polymer. Therefore, the POE6C18/PP film showed a gradual increase in the surface additive concentration because of the steady and slow migration of additives to the surface. At 4 months after extrusion, it reached a surface molar concentration of 9.75%, which was a 10-fold increase from the day 2 concentration (0.90%). In contrast, the surface additive concentration in the POE2C18/PP film reached its maximum at week 3 and stayed relatively constant between week 3 and month 4.

The POE4C18/PP film showed an interesting reversal of the migration trend during aging. Initially, the surface concentration increased, reached its maximum, and then decreased. The migration behavior of this additive is not completely understood, but it may result from the competition of various governing factors, such as surface energy minimization,[13] polymer–additive phase separation,[23] and the entropic preference of small molecules on the surface.[14,24]

Surface wettability

The addition of stearyl alcohol ethoxylate additives resulted in the alteration of the surface properties, as observed through the water contact angle. Figure 4(a) illustrates the advancing water contact angle of the PP control, POE2C18/PP, POE4C18/PP, and POE6C18/PP films measured on day 3, week 3, and month 4 after extrusion. The figures clearly demonstrate reductions in the water contact angles in all of modified films compared to the PP control and that the aging of the samples induced further improvement in the surface wettability. Because the wettability or contact angle is one of the properties

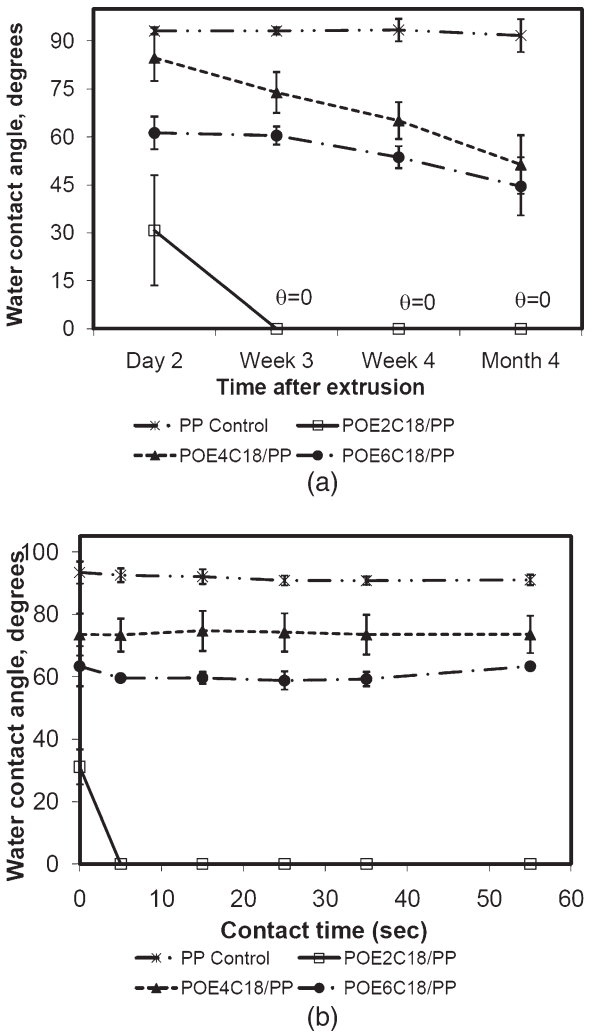

Figure 4 Water contact angles of the POE2C18/PP, POE4C18/PP, and POE6C18/PP films: (a) advancing water contact angle measurements (water contact time = 1 min) 2 days, 3 weeks, 4 weeks, and 4 months after extrusion and (b) contact angle relaxation 3 weeks after extrusion.

determined by the surface structure and composition, not by the bulk composition of the material, the reduction in the water contact angle may have been a direct effect of the surface enrichment and migration of additive molecules. Particularly, the POE2C18/PP film provided better performance in the creation of a hydrophilic surface, and this was in good agreement with the molar melt additive surface concentration, which was found to be consistently higher in the POE2C18/PP film.

Additionally, it was very interesting to observe the dynamic response of the additive-containing PP surfaces when they were brought into contact with water droplets [Fig. 4(b)]. Water droplets on the PP films almost immediately reached equilibrium, and no significant changes in the water contact angle were observed afterward. However, a reduction in the contact angle was observed as the contact time with the water droplet increased (a phenomena often recognized as *contact angle relaxation*) in the POE2C18/PP film. Indeed, when a drop of water was placed on the POE2C18/PP film surface, its contact angle, initially about 30°, started to decrease to 0° (complete wetting) within the first 5 s on contact with water.

This significant reduction of contact angle as a result of liquid contact may be evidence that the additive-containing surface was dynamic in nature, and the surface structure could respond when it was exposed to different interfacial environments. This may be attributed to a water-induced restructuring of the surface and the reaction of the surface additives with water, although we still cannot fully understand the mechanism of contact angle relaxations in additive-modified films. Possible reactions of the additive-modified surfaces on the contact of water droplets are schematically shown in Figure 5. The deposition of water droplet replaced the air/film interface with a more polar water/film interface. It may have had a minimal effect on the surface composed of homogeneous PP molecules. However, ethoxylate additives are surfactants, which are amphiphilic molecules consisting of a hydrophobic tail and a hydrophobic head, and the most favorable alignment of surfactant molecules is highly dependent on the interface character. Therefore, when air was replaced by polar water molecules, the surface conformations with the hydrophilic ethoxylated chain aligned toward water became favorable. If additives have enough mobility to realign, water droplet contact may induce restructuring of the hydrophilic head toward the water interface and increase the polarity of the surfaces, which will

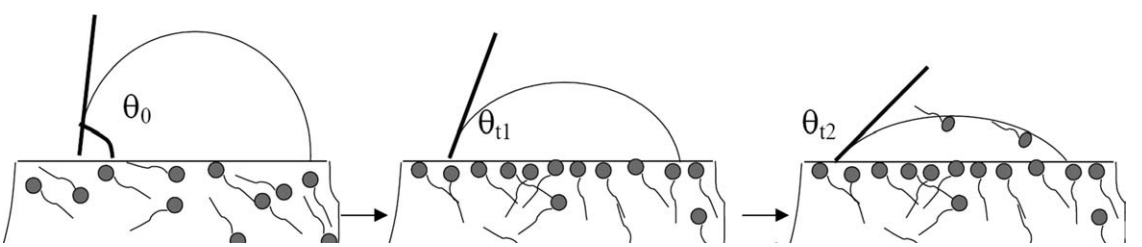

Figure 5 Schematics of the reduction on the water contact angle by the realignment and release of additives. θ_0, θ_{t1}, θ_{t2}, contact angle at contact time 0, t1, and t2 respectively.

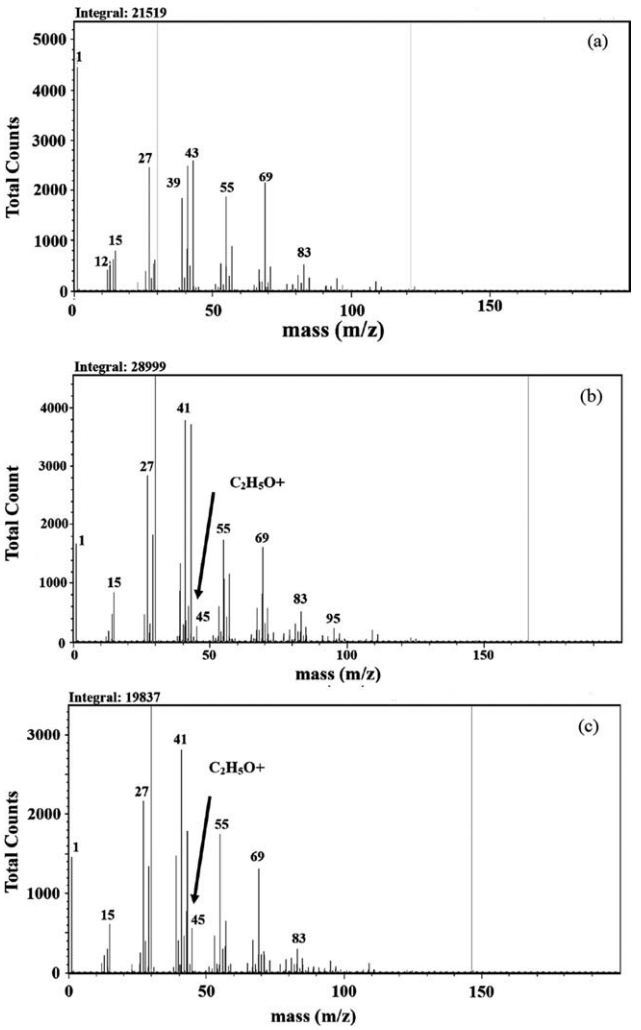

Figure 6 TOF-SIMS positive-ion mass spectra of the (a) PP control, (b) POE2C18/PP, and (c) POE6C18/PP films.

result in a reduction in the contact angles (Fig. 5). When surface additives are loosely anchored to the host polymer matrix, additives may release to the water, cause a decrease in the surface tension of water, and thus further reduce the contact angle.

Surface analysis: TOF-SIMS

XPS cannot give absolute information about the exterior surface functionalities on a fiber surface because this technique includes subsurface contributions (up to 5 nm), whereas contact angle measurements are affected by interactions between the functionalities on the outermost atomic layers of a surface fiber surface (0.5–1 nm) and the test liquid. Unfortunately the difference in analytical depth is the main reason why the surface wettability measurements cannot be fully explained from the elemental composition obtained from XPS. Therefore, TOF-SIMS, which has extreme surface sensitivity with analytical depth on the order of 1 nm, was conducted. In addition to its high surface specificity, TOF-SIMS analysis yields rich information about the chemical structure and composition of surfaces, whereas XPS mostly yields atomic compositions.[25–27]

Figure 6 shows the TOF-SIMS positive-ion spectra of the PP control, POE2C18/PP, and POE6C18/PP films for bombarding with a Ga^+ ion beam. In the spectra, characteristics secondary ions were detected, and the mass range up to $m/z = 100$ were dominated by fragments associated with both additive and PP polymer. Table IV summarizes the suggested composition of the characteristic positive secondary ions found in the samples. The signals at m/z values of 15, 27, 43, and 45 resulted from the hydrophobic and the hydrophilic segments of the additives, whereas those at m/z values of 27, 41, 43, 55, 69, and 83 were characteristic of molecular fragments associated with the PP polymer chains. In the spectra of the PP control film [Fig. 6(a)], the peaks were mostly associated with hydrocarbon fragments, and peaks corresponding to the $C_2H_5O^+$ fragment (at $m/z \approx 45$) were not found. In the case of the additive-modified films, in both POE2C18/PP [Fig. 6(b)] and POE6C18/PP [Fig. 6(c)], these segments were clearly identified at $m/z = 45$. Because $C_2H_5O^+$ fragments associate with the main components in the additive hydrophilic group (polyoxyethylene), the presence of peaks at $m/z = 45$ indicated the presence of additive on the top layer of the modified film. Furthermore, on the basis of the high sensitivity of TOF-SIMS, this may indicate the presence of hydrophilic groups directly aligned toward to the surface, which altered the surface hydrophilicity.[27]

Then, the surface distribution of the hydrophilic ethoxylate chain segment in the melt additives was, therefore, determined by the mapping of the molecular fragment C_2H_5O+ at the identified $m/z = 45$. Because we believe that the presence of a segregated stearyl alcohol ethoxylated chain greatly influenced the surface composition of the modified PP films, the presence and orientation of the hydrophilic segment affected the water contact angle measurements. The distribution of the hydrophilic polyoxyethylene

TABLE IV
Suggested Structure of the Characteristic Positive Secondary Ions Emitted from the Melt-Additive-Modified PP Films

Mass (m/z)	Fragment composition
15	CH_3+
27	C_2H_3+
41	C_3H_5+
43	C_2H_3O+, C_3H_7+
45	C_2H_5O+
55	C_4H_7+
69	C_5H_9+
83	$C_6H_{11}+$

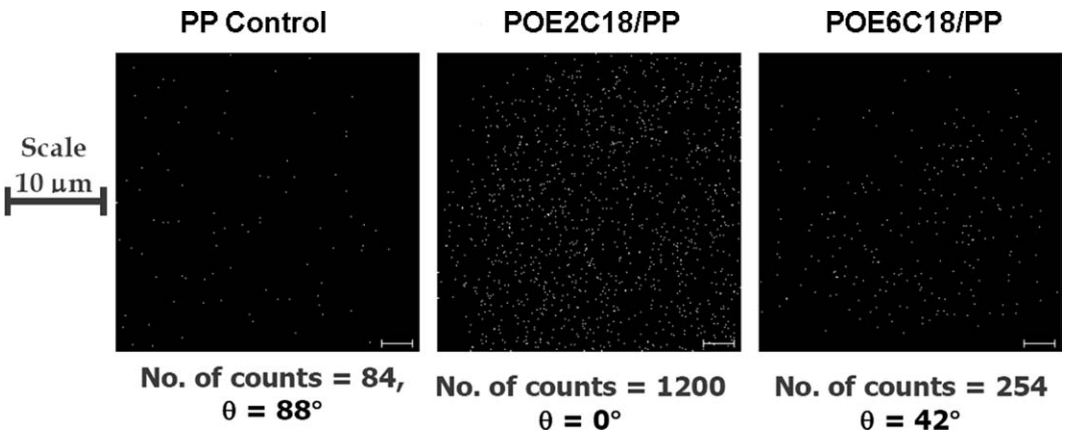

Figure 7 Characteristic secondary-ion images of C_2H_5O+ ($m/z = 45$) fragments in the PP control and surface-modified PP films with stearyl alcohol ethoxylate melt additives (100 μm × 100 μm area). In the subscript of each map, the maximum number of counts per pixel and the equilibrium water contact angles are given.

segment of the additive on the topmost surface mapped with the TOF-SIMS technique in the imaging analysis mode is illustrated in Figure 7. There were few to no polyoxyethylene fragments in the PP polymer, whereas the presence of a significant amount of polyoxyethylene fragments observed in the POE2C18/PP and POE6C18/PP films indicated the presence or the migration of the melt additives to the air–polymer interface, and they are more intense for the POE2C18/PP film compared to the POE6C18 film. This may have reflected the more polar nature of the POE2C18/PP film's top most surface and its high wettability.

Surface morphology: AFM

The AFM images revealed changes in the surface morphology caused by the melt blending of additives through surface heterogeneity and microphase separation (Fig. 8). The AFM images of the PP control film [Fig. 8(a)] showed a typical spherulitic crystalline structure, which indicated the initiation of crystallization from several nuclei distributed on the sample surface. The spherulite crystalline structures were also observed in the additive-containing samples, and this may have indicated that the additives did not disturb the crystalline structure of the samples.

Even the spherulite crystalline morphology was preserved, the surface became less structured because of the presence of additives at the surfaces, and the surface topography was rough and dominated by the presence of a variety of nonuniform features. Ridgelike structures were apparent on the spherulite crystalline surface in the POE2C18/PP film [Fig. 8(b)]. They were more clear in the height profiles (Fig. 9). Compared to the height profile of the PP controls [Fig. 9(a)], which had relatively smooth spherulite surfaces, a series of peaks and valleys with a peak-to-peak distance ranging from 500 nm to 1.5 μm existed on the POE2C18/PP film surfaces [Fig. 9(b)]. We do not fully understand the reasons for these unique textures, but they may have been the result of arrangements of melt additives in the surface. The POE4C18/PP and POE6C18/PP films also exhibited these ridgelike structures, which confirmed that the ethoxylate additives altered the surface structures of the PP films [Fig. 8(c,d)]. In case of the POE4C18/PP modified films, in addition to the ridge structure, relatively large size bumps with a bump height of up to 2 μ were present and led to increasing surface roughness. Both the root-mean-square roughness and roughness factor, shown in Table V, indicated that the presence of bumps in the POE4C18/PP film led to rough surfaces, whereas the POE2C18/PP and POE6C18/PP film showed only small changes in surface roughness.

The wetting behavior of a planar surface is affected by both the material's surface chemistry and its local geometry or roughness; it is possible that morphological changes in the surfaces in the melt-additive-containing samples affected the water contact angles. However, the relatively small changes in the roughness factor, which is defined as the ratio of the true surface area to the planar projected area of the surface and is possible indicator of rough surface contact angle alteration, indicated that the contribution of roughness to the surface wettability may have been insignificant compared to the contribution of the surface composition changes observed through XPS and TOF-SIMS observation.[28,29]

Water immersion durability

The study of the surface wettability behavior of the PP films containing additives by means of contact angle relaxation phenomena established that the

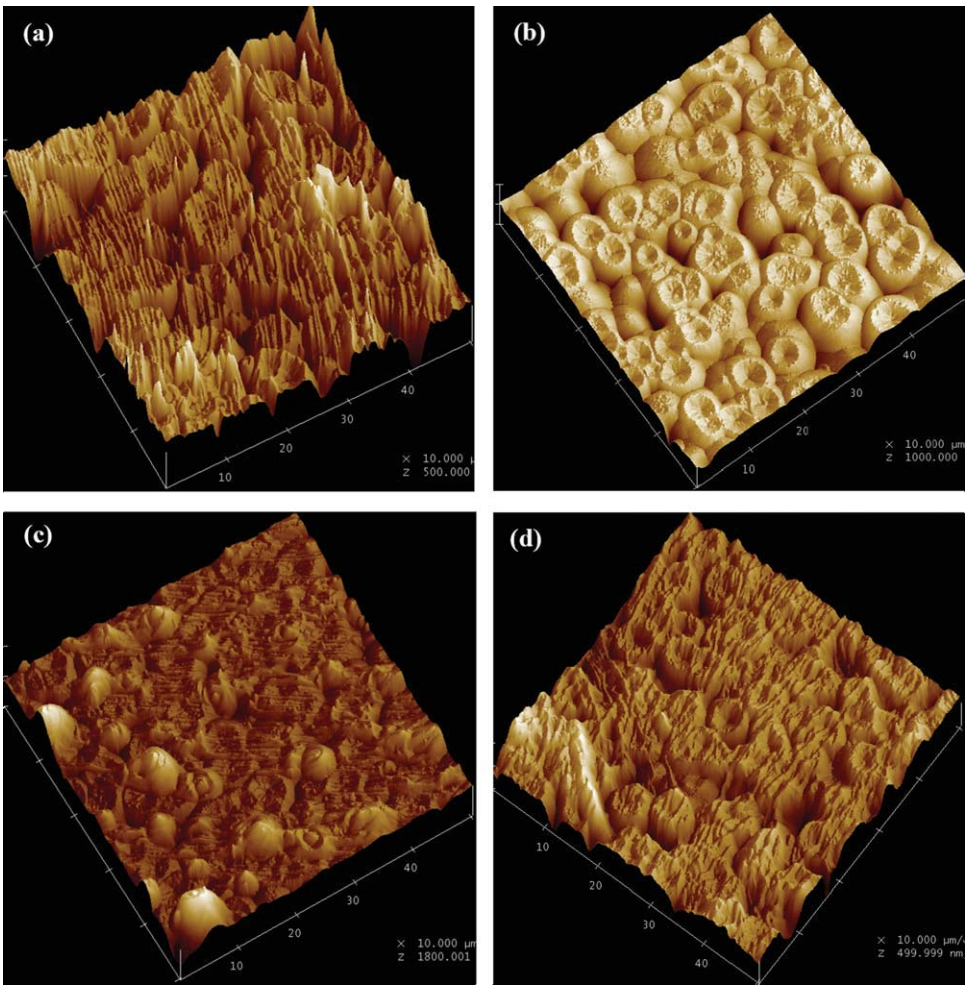

Figure 8 AFM images of sample surfaces: (a) PP control, (b) POE2C18/PP, (c) POE4C18/PP, and (d) POE6C18/PP (>4 months after extrusion). [Color figure can be viewed in the online issue, which is available at wileyonlinelibrary.com.]

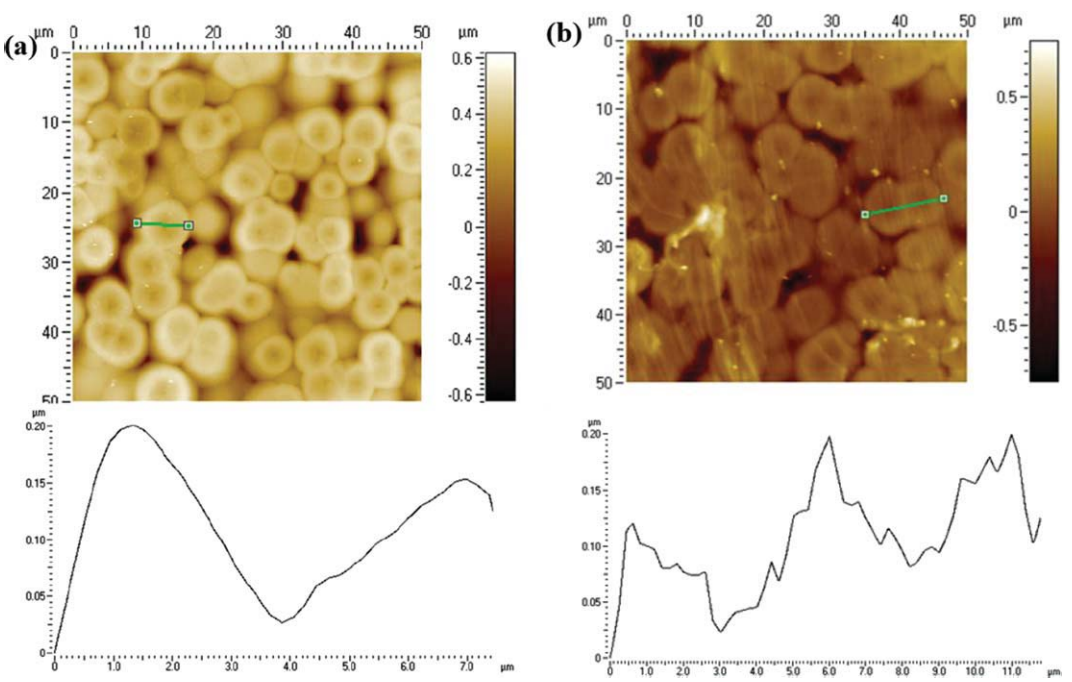

Figure 9 Height profiles of AFM images of the (a) PP control film surfaces and (b) POE2C18/PP film surfaces (>4 months after extrusion). [Color figure can be viewed in the online issue, which is available at wileyonlinelibrary.com.]

TABLE V
Surface Roughness of the PP Control and Modified PP Films More Than 4 Months After Extrusion

Material	Root-mean-square roughness (nm) on 50 × 50 nm^2	Roughness factor
PP control	128	1.0124
POE2C18/PP	137	1.0176
POE4C18/PP	358	1.0576
POE6C18/PP	111	1.0104

contact of water altered the surfaces by reconstruction to minimize the surface energy of the interface. Then, the response of the surfaces to contact with water was further studied by the immersion of the ethoxylated modified PP films. The PP/additive surface response to prolonged exposure to water and the degree of surface alteration were affected by ethoxylate chain length.

Changes in the surface O/C ratio (%) before and after 6 h of water immersion are illustrated in Figure 10. This figure indicates a significant decrease in the surface oxygen concentration in the POE6C18/PP film surfaces, whereas the surface oxygen concentrations in the POE2C18/PP and POE4C18/PP films increased. The results shown in Figure 10 agree well with the surface wettability measurements illustrated in Figure 11. As explained before, the POE6C18 additive was more hydrophilic in nature, so the PP films incorporated with the POE6C18 additive demonstrated the loss of surface hydrophilicity, which resulted in an increase in the water contact angle after 6 and 24 h of water immersion. However, the PP films with the POE4C18 additive became more hydrophilic, and significant reductions in the water contact angle after 6, 12, and 24 h water immersion were observed. Thermodynamically

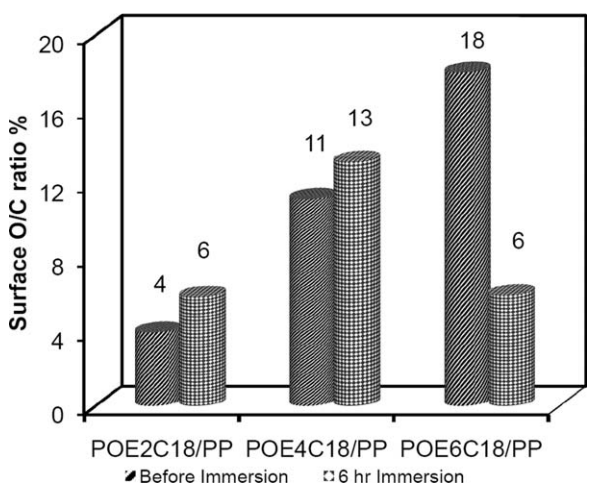

Figure 10 Surface O/C ratios (%) of the PP films modified with ethoxylated melt additives before and after 6 h of water immersion (at 4 months after extrusion).

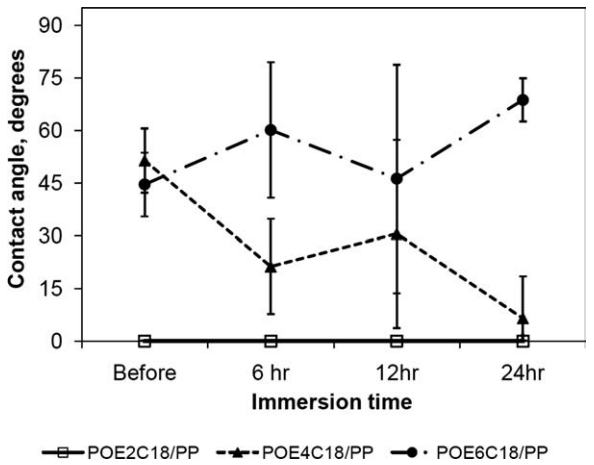

Figure 11 Water contact angles before and after 6, 12, and 24 h of water immersion of the surface-modified PP films (at 4 months after extrusion).

modified PP/additive surfaces preferred a water interface to an air interface; therefore, prolonged exposure to water during the immersion tests may have resulted in additional additive migration and/or realignment to the PP surface.

With the object of confirming whether or not the loss of surface oxygen concentration or, in other words, the loss of surface additive molecules happened during water immersion, we analyzed the water samples used for soaking the PP films containing POE2C18 and POE6C18 additives for changes in the water surface tension (Fig. 12). This clearly showed evidence for the release of surface-additive molecules into water, as represented by a reduction in the surface tension of water with immersion time. The surface tension analysis reported also supported the assumption made before for contact angle relaxation that additives with poor anchoring capabilities may actually have released into the water droplet placed on the PP film and further decreased the water contact angle by a reduction in the water surface tension.

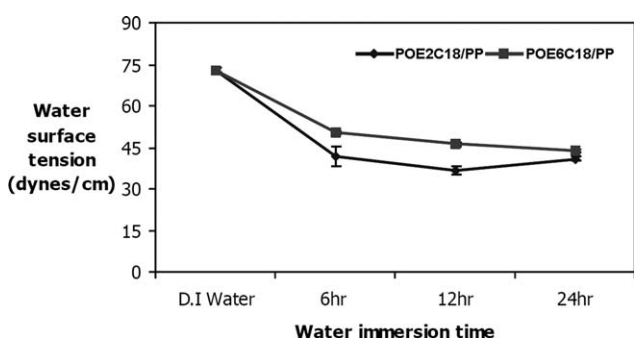

Figure 12 Surface tension (dyn/cm) of water before and after the soaking of the POE2C18/PP and POE6C18/PP films for 6, 12, and 24 h (at 4 months after extrusion).

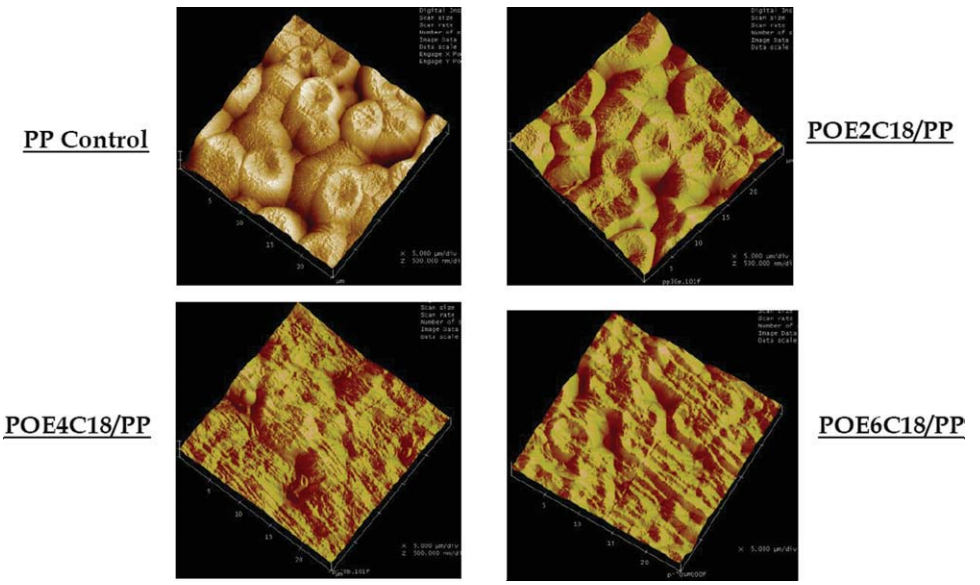

Figure 13 Third-dimensional AFM surface plots of the PP control and modified PP films after 6 h of water immersion (>4 months after extrusion). [Color figure can be viewed in the online issue, which is available at wileyonlinelibrary.com.]

The alteration of the additive-containing surface was verified through AFM images (Fig. 13). Although water immersion induced few changes in the PP control surface, a significant reduction in the surface roughness accompanied by the erosion of irregular surface features was observed in the additive-containing PP surfaces after water immersion.

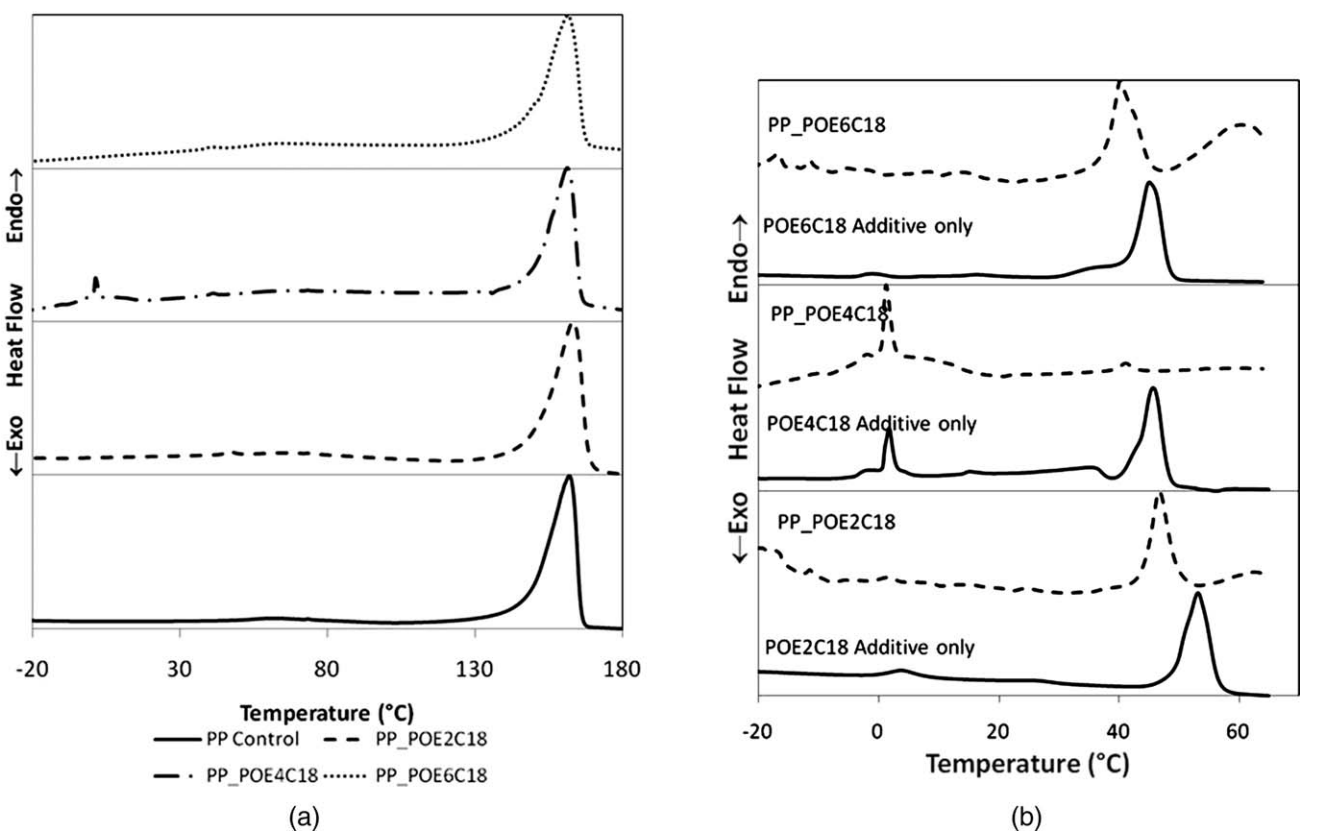

Figure 14 (a) DSC thermograms of the surface-modified PP films with melt additives and (b) the melt additive melting behavior (DSC thermograms from −20 to 70°C) in these films in comparison with pure melt additives (the heat flow is not to scale).

TABLE VI
Melting Temperatures and Crystallinity of the Melt Additives and Modified PP Films with Melt Additives

Sample	Melting temperature (°C) Melt additive			PP	Crystallinity (%)
POE2C18	4	26	53		
POE4C18	2	15	46		
POE6C18	45				
PP control				162	43.0
POE2C18/PP	47	73		163	43.2
POE4C18/PP	−2	2	41	161	33.0
POE6C18/PP	40	73		162	37.8

DSC analysis and crystallinity

The DSC thermograms of the PP/additive films (Fig. 14) revealed that the modified PP films with the melt additives exhibited multiple melting endotherms. In all samples, the dominant endothermic peaks corresponded to the melting of the PP component, but a series of small endothermic peaks were also detected at temperatures close to the melt points of the melt additives [Fig. 14(b)], although these are not clearly visible in Figure 14(a). This indicated that the PP/melt additive films formed phase-segregated polymer blends. Table VI summarizes the thermal properties observed by DSC for the PP films modified with the melt additives compared with those of the additives.

Major melting peaks for all of the modified PP films were caused by PP crystal melting observed about at 160°C, and this was because of the high composition of PP in the films. There were no significant changes were observed in the melting behavior of the PP components in the blends [Fig. 14(a) and Table VI]. The onset melting temperatures were almost identical in all of the films, regardless of the presence and types of additives, although slight reductions in PP crystallinity were observed in POE4C18/PP and POE2C18/PP. The melting temperature and percentage crystallinity of PP showed no appreciable changes in the melt-blended films. These were good indications that thermal properties and crystalline structure of the base PP polymer were not influenced by the addition of nonionic melt additives. This was also supported by AFM observations. which showed the preservation of spherulite crystalline structures in the additive-modified films (Fig. 8).

The melting endotherms corresponding to the melting of the additives were not so obvious, mostly because there was only small amount of melt additive present in the films. However, when the DSC curves of the temperature ranges of interest were magnified, as shown in Figure 14(b), distinct melting peaks of the additives were observed. The DSC thermograms of the additives only are also given in Figure 14(b) for comparison. They showed broad melting ranges and indicated crystals that coexisted and came in a range of sizes and types and with various degrees of perfection. Those multiple melting peaks were also attributed to the inhomogeneity of the additives revealed by HPLC analysis (Fig. 1). As previously discussed, all three additives showed polydispersity with ethoxylated chain length distributions, and this may have contributed to the formation of inhomogeneous crystals. In the additive/PP films, most of these peaks were still present, but significant shifts of melting points were observed, and also some melting peaks disappeared. This indicated interactions between the PP polymer and the melt additive.

CONCLUSIONS

The surface segregation behavior of ethoxylated melt additives and their role in the modification of the PP surface were discussed. XPS measurements revealed the surface enrichment of oxygen (or melt additives) in the melt-blended PP samples. The melt additive surface concentration changed as a function of time and indicated the ongoing migration behavior after extrusion.

A substantial reduction in the water contact angles over time indicated that the increase in wettability was dependent on the polarity of the modified surface. The top surface additive structure, analyzed with TOF-SIMS, showed good agreement with the water contact angle measurements. The presence of a high additive concentration in the surfaces changed the morphology of the surfaces and created more rough surfaces.

Immersion into water changed the surface properties; this depended on the type of melt additive and the immersion time. The release of additive molecules into water when the sample was immersed in water were observed via a reduction in the water surface tension.

The authors express their gratitude to Goulston Technologies and the Analytical Instrumentation Facility (North Carolina State University) for their assistance and support of this project.

References

1. Yilgör, E.; Yilgör, I.; Süzer, S. Polymer 2003, 44, 7271.
2. Nonwoven Textiles 1997–2007 World Survey; TECNON: London, UK, 2000.
3. Ewen, M.; Peter, K.; Hocker, H.; Reichelt, N.; Patzsch, M. Chem Fibers Int 1998, 48, 383.
4. Witte, J. D. Nonwovens World 2001, 10, 97.
5. Chung, T. C.; Lee, S. H. J Appl Polym Sci 1997, 64, 567.
6. Karger-Kocsis, J. Polypropylene: An A–Z Reference; Kluwer: Dordrecht, 1999.
7. Chan, C. M. Polymer Surface Modification and Characterization; Hanser Gardner: Munich, 1994; p 225.

8. Yamada, K.; Kimura, J.; Hirata, M. J Appl Polym Sci 2003, 87, 2244.
9. Yang, Q.; Xu, Z.-K.; Dai, Z.-W.; Wnag, J.-L.; Ulbricht, M. Chem Mater 2005, 17, 3050.
10. Ratzsch, M.; Arnold, M.; Borsig, E.; Bucka, H.; Reichelt, N. Prog Polym Sci 2002, 27, 1195.
11. Datla, V. M. Ph.D. Dissertation, North Carolina State University, 2007.
12. Witte, J. D. Nonwovens World 2001, 10, 97.
13. Lee, H.; Archer, L. A. Macromolecules 2001, 34, 4572.
14. Tanaka, K.; Takahara, A.; Kajiyama, T. Macromolecules 1998, 31, 863.
15. Griffin, W. C. J Soc Cosmet Chem 1954, 5, 259.
16. Lee, H.; Archer, L. A. Polymer 2002, 43, 2721.
17. Sachin, S. N.; Devi, S.; Rao, G. S. S.; Rao, K. V. J Appl Polym Sci 1996, 61, 97.
18. Wagner, C. D.; Davis, L. E.; Zeller, M. V.; Taylor, J. A.; Raymond, R. H.; Gale, L. H. Surf Interface Anal 1981, 3, 211.
19. Handbook of X-Ray Spectrometry: Methods and Techniques; Grieken, R.; Markowicz, A., Eds.; Marcel Dekker: New York, 1993.
20. Ladhe, A. R.; Radomyselski, A. R.; Bhattacharyya, D. Langmuir 2006, 22, 615.
21. Rissler, K. J Chromatogr 1996, 742, 1.
22. Chen, X.; Gardella, J. A. Macromolecules 1992, 25, 6621.
23. Shonaike, G. O.; Simon, G. P. Polymer Blends and Alloys; Marcel Dekker: New York, 1999; p 1.
24. Kumar, S. K.; Russell, T. P. Macromolecules 1991, 24, 3816.
25. Belu, A. M.; Graham, D. J.; Castner, D. G. Biomaterials 2003, 24, 3635.
26. Weng, L.-T.; Chan, C.-M. Appl Surf Sci 2006, 252, 6570.
27. Briggs, D.; Brewis, D. M.; Dahm, R. H.; Fletcher, I. W. Surf Interface Anal 2003, 35, 156.
28. Wenzel, R. N. Ind Eng Chem 1936, 28, 988.
29. Wenzel, R. N. J Phys Chem 1949, 53, 1466.